ELSEVIER

European Journal of Pharmacology 338 (1997) 159–169

ejp

Pharmacological characterization of the vesamicol analogue (+)-[^{125}I]MIBT in primate brain

Julie K. Staley [a], Deborah C. Mash [a], Stanley M. Parsons [b], Anil B. Khare [c], Simon M.N. Efange [c,*]

[a] *Departments of Neurology and Molecular and Cellular Pharmacology, University of Miami School of Medicine, Miami, FL 33101, USA*
[b] *Department of Chemistry and the Graduate Program in Biochemistry and Molecular Biology, University of California, Santa Barbara, CA 93106, USA*
[c] *Departments of Radiology, Medicinal Chemistry and Neurosurgery, University of Minnesota, Minneapolis, MN 55455, USA*

Received 18 August 1997; accepted 29 August 1997

Abstract

The vesamicol analogue, *meta*-[^{125}I]iodobenzyltrozamicol [(+)-[^{125}I]MIBT] was evaluated as a probe for the in vitro labeling of the vesicular acetylcholine transporter in primate brain. In the striatum, (+)-[^{125}I]MIBT bound a single high-affinity site with a K_d value of 4.4 ± 0.7 nM. Competition for (+)-[^{125}I]MIBT binding to the striatum by a group of vesamicol analogues displayed a pharmacological profile similar to the rank order of potency previously observed for the vesicular acetylcholine transporter on *Torpedo* synaptic vesicles. High-affinity binding of (+)-[^{125}I]MIBT in the occipital cortex was characterized by a K_d value of 4.6 ± 1.1 nM. However, the rank order of potency for inhibition of (+)-[^{125}I]MIBT binding to the occipital cortex by the same test compounds differed from that observed in the striatum. The results suggest that (+)-[^{125}I]MIBT is a reliable probe of the vesicular acetylcholine transporter in primate striatum, but its binding in primate occipital cortex is more complex. © 1997 Elsevier Science B.V.

Keywords: Vesamicol receptor; Acetylcholine; Synaptic vesicle; Acetylcholine transporter, vesicular

1. Introduction

Historically, cholinergic nerve terminals have been distinguished by the phenotypic expression of choline acetyltransferase, the Na^+-dependent high-affinity choline transporter and acetylcholinesterase. The recent identification and cloning of the vesicular acetylcholine transporter provides yet another marker for the cholinergic system. Recent molecular cloning studies have revealed that the full coding region of the vesicular acetylcholine transporter is 'nested' within the first intron of the choline acetyltransferase gene locus, suggesting that the expression of both choline acetyltransferase and vesicular acetylcholine transporter are closely linked to each other (Erickson et al., 1994; Bejanin et al., 1994; Roghani et al., 1994).

Immunohistochemical studies have demonstrated that the vesicular acetylcholine transporter is localized to synaptic vesicles within cholinergic terminals (Gilmor et al., 1996; Weihe et al., 1996). Pharmacologically, the vesicular acetylcholine transporter is identified by the high-affinity binding of (−)-*trans*-2-(4-phenylpiperidino)cyclohexanol (vesamicol; Fig. 1; Bahr and Parsons, 1986b), a potent noncompetitive inhibitor of acetylcholine uptake into purified cholinergic synaptic vesicles isolated from the electric organ of the marine ray Torpedo (Anderson et al., 1983; Bahr and Parsons, 1986a). Vesamicol also acts on purified rat brain synaptic vesicles (Haigh et al., 1994) and many intact or semi-intact neural preparations to block the refilling of recycling synaptic vesicles (VP_2) with acetylcholine (Ricny and Whittaker, 1993). With the discovery of this marker protein, efforts have been initiated to investigate its potential for assessing the integrity of cholinergic nerve terminals in neurodegenerative diseases characterized by reduced cholinergic function.

In early studies with [^{3}H]vesamicol (Marien et al., 1987; Altar and Marien, 1988), in vitro autoradiography demonstrated a labeling pattern that parallels the distribution of cholinergic nerve terminals (Stavinoha et al., 1974;

* Corresponding author. Department of Radiology (Mayo Box 292), University of Minnesota Hospital and Clinic, 420 Delaware Street S.E., Minneapolis, MN 55455, USA. Tel.: (1-612) 626-6646; Fax: (1-612) 624-8495.

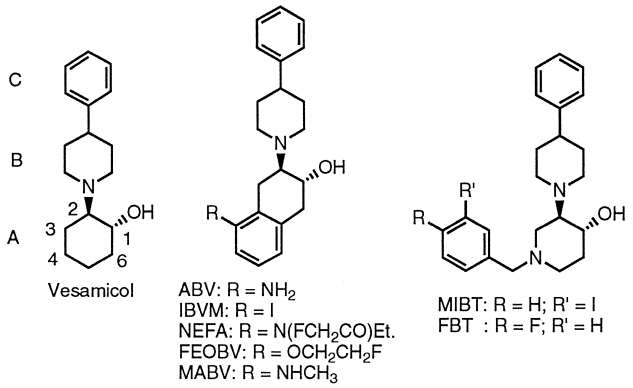

Fig. 1. Molecular structure of (−)-vesamicol and selected VR ligands.

Mesulam et al., 1983; Quirion, 1987). Nevertheless, subsequent studies of [^{3}H]vesamicol binding to membrane preparations obtained from brain regions having cholinergic deficits yielded puzzling results. In the rat brain, Marien et al. (1987) and Altar and Marien (1988) reported a 33% decrease in hippocampal binding of [^{3}H]vesamicol following the transection of the fimbria. However, hippocampal choline acetyltransferase levels were decreased by 61%. Subsequently, Ruberg et al. (1990) and Holley et al. (1993) reported finding no change in [^{3}H]vesamicol binding in rat cortex following a chemical lesion of the nucleus basalis. In addition, changes in the binding of [^{3}H]vesamicol in Alzheimer's disease brain post mortem did not correlate with changes in the amounts of choline acetyltransferase and acetylcholinesterase (Kish et al., 1990; Ruberg et al., 1990). In the frontal cortex, [^{3}H]vesamicol binding was reduced by 17–35% while choline acetyltransferase levels were decreased by 54%. Moreover, [^{3}H]vesamicol binding in the temporal cortex was increased by 26–37%, in spite of a 30–50% reduction in choline acetyltransferase levels.

To explain the apparent discrepancies, a number of hypotheses were advanced, including the following: (1) that cholinergic neurons that survive the lesion might compensate by expressing higher levels of synaptic vesicles; (2) that one segment of surviving cholinergic terminals might express inadequate levels of choline acetyltransferase and acetylcholinesterase; (3) that degenerating (choline acetyltransferase-deficient) cholinergic terminals might exhibit up-regulation of the vesicular acetylcholine transporter; and (4) that a substantial fraction of [^{3}H]vesamicol binding sites might be associated with non-cholinergic elements. In support of the latter hypothesis, vesamicol was found to exhibit nanomolar affinity for σ sites (Efange et al., 1992).

The poor selectivity of (−)-vesamicol in mammalian brain prompted a search for more potent and selective ligands that could facilitate the mapping of cholinergic terminals in vitro and in vivo (Kilbourn et al., 1990; Rogers and Parsons, 1990; Mulholland et al., 1992; Rogers et al., 1992; Van Dort et al., 1993; Kuhl et al., 1994; Shiba et al., 1996). This report describes the pharmacological characterization of the binding of one such ligand, (+)-*meta*-[^{125}I]iodobenzyltrozamicol ((+)-[^{125}I]MIBT, Fig. 1) (Efange et al., 1993b).

2. Materials and methods

2.1. Tissue specimens

Monkey (*Macaca mulatta*) brain specimens (from three 5 kg males) were obtained from Perrine Primate Center in Miami, Florida. The animals were restrained with ketamine, deeply anesthetized with halothane gas and placed in a stereotaxic headholder. Following removal of the calvarium and upper cervical vertebra, cardiopulmonary arrest was induced by medullary transection. The brain was rapidly removed and frozen in 2-methylbutane at −30°C. For in vitro binding assays, tissue punches were taken from the striatum and occipital cortex.

2.2. Radioligands and drugs

(+)-[^{125}I]MIBT (specific activity = 1500 ± 200 Ci/mmol) was synthesized as described previously (Efange et al., 1993b). [^{3}H]vesamicol (specific activity = 50.5 Ci/mmol) was obtained from NEN Dupont (Wilmington, DE, USA). Racemic *meta*-iodobenzyltrozamicol, *para*-fluorobenzyltrozamicol, and 5-aminobenzovesamicol were synthesized as described previously (Rogers et al., 1989; Efange et al., 1993a). The pure enantiomers were obtained by chromatographic resolution on a 250 mm × 10 mm id Chiralcel OD column (Chiral Technologies, Exton, PA, USA) operating at a flow rate of 2.4 ml/min with a mobile phase of isopropyl alcohol–hexane. Haloperidol and (+)- and (−)-vesamicol were purchased from Research Biochemicals International (Natick, MA, USA). The enantiomers of pentazocine were provided by the National Institute on Drug Abuse.

2.3. Binding assays

All binding assays were carried out in a buffer containing 50 mM Tris, pH 7.6, with 120 mM NaCl, 5 mM KCl, 2 mM $CaCl_2$, 1 mM $MgCl_2$ and 0.5% bovine serum albumin. A coating of Sigmacote (Sigma, St. Louis, MO, USA) was applied to all test tubes, pipet tips and beakers prior to use in order to prevent binding of vesamicol analogues to container surfaces (Rogers and Parsons, 1993). Membranes (from striatum or occipital cortex) for in vitro binding assays were prepared by homogenizing the tissue using a Brinkman polytron at setting 3 for 15 s in 20 vol of ice-cold assay buffer without bovine serum albumin. Membrane pellets were obtained by centrifugation at 15 000 × *g* for 15 min, washed once and resuspended to a final concentration of 5 mg/ml and 15 mg/ml for (+)-

[^{125}I]MIBT and [^{3}H]vesamicol binding assays, respectively.

The rates of association and dissociation kinetics of (+)-[^{125}I]MIBT were determined at 25°C using a radioligand concentration of 0.07 nM in the presence or absence of 10 μM (±)-5- aminobenzovesamicol. For the association rate, aliquots (2 ml) of the assay medium were filtered through Whatman 934AH filters presoaked in 0.1% polyethyleneimine at selected intervals following the addition of the radiotracer. The filters were washed 3 times with 4.5 ml of ice-cold buffer. Upon establishing equilibrium (60 min), dissociation of (+)-[^{125}I]MIBT was initiated by the addition of 1 μM *meta*-iodobenzyltrozamicol or by a 50-fold dilution of a 10-fold concentrated suspension with assay buffer maintained at room temperature. Aliquots (2 or 10 ml, respectively) were then removed and filtered at the specified times to determine the rate of (+)-[^{125}I]MIBT dissociation.

For saturation analyses, membranes (5 mg/ml) were incubated with 0.07 nM (+)-[^{125}I]MIBT in the presence of increasing concentrations of unlabeled (+)-*meta*-iodobenzyltrozamicol (0.01 to 1000 nM) in a final volume of 2 ml. Nonspecific binding was defined as the disintegrations per minute bound in the presence of 1 μM (+)-*meta*-iodobenzyltrozamicol or 10 μM (±)-5-aminobenzovesamicol. At the end of the incubation period (1 h at 25°C), each sample was diluted with 9 ml of cold buffer for one min and filtered under reduced pressure through Whatman 934AH filters presoaked in 0.1% polyethyleneimine. Filters were washed 3 times with 4.5 ml of cold buffer. The total radioligand bound was determined by counting filters in a Packard Gamma counter at 75% efficiency.

For competition studies, various concentrations of the selected competing ligands were incubated with membranes (5 mg/ml) in the presence of 0.07 nM (+)-[^{125}I]MIBT, for 1 h, at 25°C in a final volume of 1 ml. Bound (+)-[^{125}I]MIBT was separated from free radioligand by vacuum filtration, and filters were counted as described for the saturation studies. For [^{3}H]vesamicol binding assays, competing ligands were incubated with 5 nM [^{3}H]vesamicol and membranes (15 mg/ml) for 1 h at 25°C. Each sample was diluted with 4 ml of ice-cold buffer and filtered through Whatman 934AH filters presoaked in 0.1% polyethyleneimine. The filters were washed 3 times with 4 ml of ice-cold buffer. Filters were soaked in Cytoscint cocktail overnight and counted on a Beckman Scintillation counter at 50% efficiency.

2.4. Data analysis

Saturation binding data was analyzed using the COLD program of EBDA (Elsevier, Biosoft). The affinity and density values were defined by the iterative, nonlinear curve fitting program LIGAND. The Hill slopes and K_i values for the competitors were obtained using DRUG (EBDA) and LIGAND. The association and dissociation rate constants were determined by KINETIC (Elsevier, Biosoft). For all studies, a partial F test was used to determine if a one-site model fit the data adequately or whether a two-site model was justified. The data are presented as two significant figures of the mean ± S.E. of two to four experiments.

3. Results

3.1. Characterization of (+)-[^{125}I]MIBT binding in primate striatum: comparison with [^{3}H]vesamicol binding

Binding of (+)-[^{125}I]MIBT to striatal membrane homogenates was rapid and reversible. Equilibrium was established within 20 min at 25°C (Fig. 2A). Statistical analysis revealed a biphasic association curve, with mean association rate constants of (k_{obs}) of 4.9 ± 1.0 and 0.5 ± 0.3 min^{-1}, respectively ($n = 3$, $p < 0.05$). The fast and slow components of association accounted for 70% and 30% of the specifically bound (+)-[^{125}I]MIBT, respectively. Dissociation of (+)-[^{125}I]MIBT from striatal membranes was also biphasic (Fig. 2B). In the presence of 1 μM (+)-*meta*-iodobenzyltrozamicol, 70% of the specifically bound (+)-[^{125}I]MIBT dissociated with an apparent rate constant of 1.1 ± 0.4 min^{-1} and 30% dissociated with a rate constant of 0.0012 ± 0.003 min^{-1} ($n = 4$, $p < 0.001$). Dissociation of (+)-[^{125}I]MIBT initiated by a 50-fold dilution with assay buffer (25°C) provided similar dissociation rate constants (data not shown).

Binding of (+)-[^{125}I]MIBT to membrane homogenates from primate striatum was saturable (Fig. 3A). Specific binding was consistently found to constitute 60% of the total binding in the presence of 10 μM (±)-5-aminobenzovesamicol and 70% in the presence of 1 μM unlabeled (+)-*meta*-iodobenzyltrozamicol. (−)-5-Aminobenzovesamicol has been previously shown to demonstrate very high affinity for the vesicular acetylcholine transporter in *Torpedo* synaptic vesicles (Rogers et al., 1993). When the nonspecific binding was defined with 10 μM (±)-5-aminobenzovesamicol, a single population of binding sites was observed (Fig. 3A). This site was characterized by a mean dissociation constant (K_d) of 4.4 ± 0.7 nM and a density (B_{max}) of 41 ± 7.0 pmol/g (obtained from five independent determinations). In contrast, a markedly curvilinear Rosenthal plot (Fig. 3B) was obtained when the nonspecific binding was determined with 1 μM unlabeled (+)-*meta*-iodobenzyltrozamicol. Iterative curve fitting with LIGAND revealed a high- and a low-affinity binding site, with K_d values of 3.9 ± 0.5 and 160 ± 66 nM, respectively ($n = 5$; $p = 0.0001$). The corresponding B_{max} values were 38 ± 11 and 160 ± 17 pmol/g tissue, respectively.

Pharmacological characterization of the binding of (+)-[^{125}I]MIBT to striatal membranes is illustrated in Fig. 4A and summarized in Table 1. A low concentration of (+)-

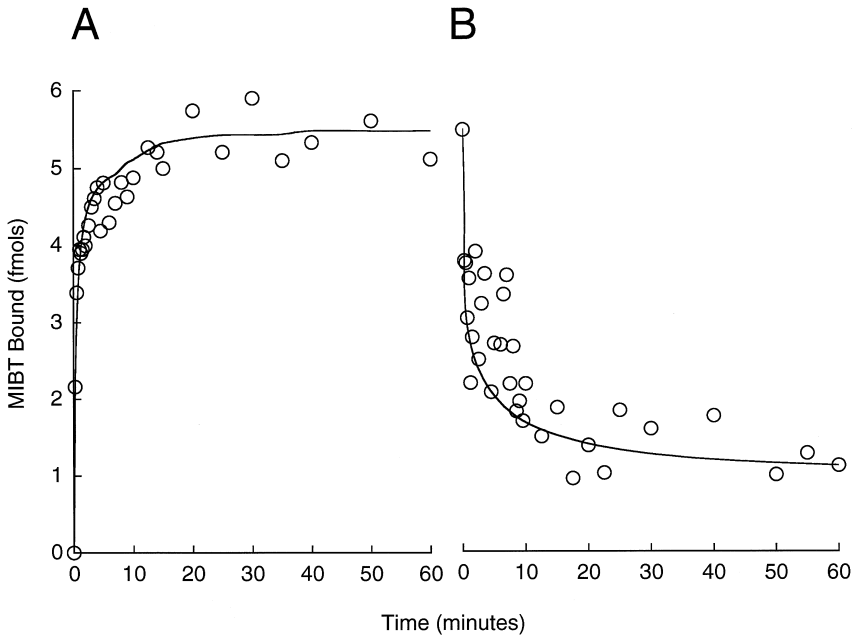

Fig. 2. Kinetic analysis of [^{125}I]-(+)-MIBT binding to primate striatum. (A) Association of [^{125}I]-(+)-MIBT (0.07 nM) to membrane homogenates from the striatum. Analysis of the data with KINETIC (Biosoft) indicated the data best fit a two site model with $t_{1/2}$ values of 0.2 min and 1.4 min, respectively. (B) Dissociation of [^{125}I]-(+)-MIBT from membranes homogenates from the striatum. After equilibrium was established, dissociation was initiated by the addition of 1 μM (+)-*meta*-iodobenzyltrozamicol or a 50-fold dilution with room temperature buffer and aliquots were removed at the indicated time points. Regardless of the method by which dissociation was initiated, a biphasic model of (+)-[^{125}I]MIBT dissociation, with $t_{1/2}$ values of 0.6 min and 57.8 min, was statistically preferred. Shown here is the average of 4 independent determinations.

[^{125}I]MIBT (0.07 nM) was used in order to selectively label the high-affinity binding site. At this concentration, 90% of the bound (+)-[^{125}I]MIBT occupied the high-affinity site and only 10% occupied the low-affinity site. Vesamicol and the structurally-related vesicular acetylcholine transporter ligands were the most potent inhibitors

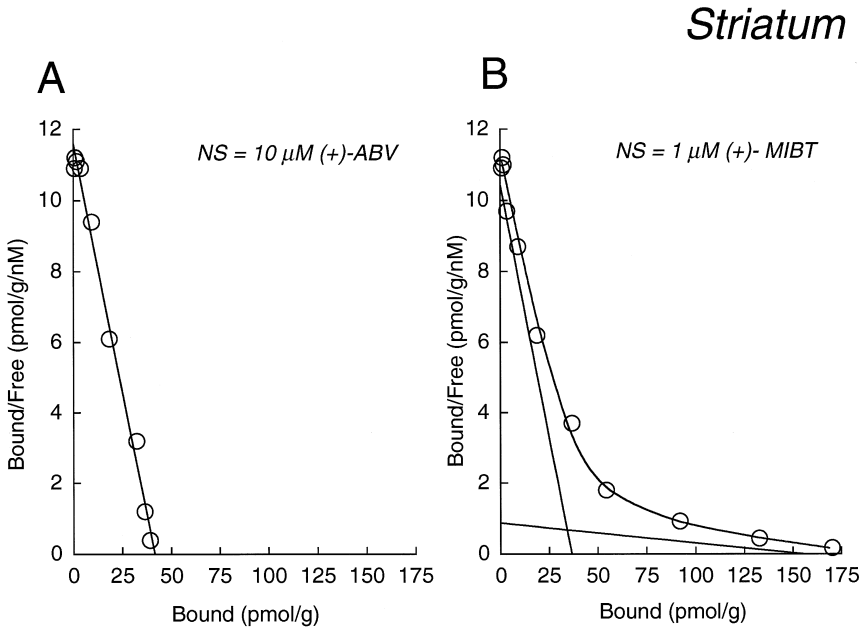

Fig. 3. Cold saturation analysis of (+)-[^{125}I]MIBT binding to a primate striatum. Striatal membrane homogenates were incubated with (+)-[^{125}I]MIBT in the presence of increasing concentrations of unlabeled (+)-*meta*-iodobenzyltrozamicol for 1 h at 25°C. Illustrated here is a representative experiment assayed in triplicate. The data were analyzed with the EBDA/LIGAND program for binding analysis. (A) Rosenthal plot observed when nonspecific binding was defined using 10 μM (±)-5-aminobenzovesamicol. Note that binding was linear with a K_d value of 3.7 nM and a B_{max} value of 41.7 pmol/g for this representative subject. (B) Rosenthal plot observed when nonspecific binding was defined using 1 μM (+)-*meta*-iodobenzyltrozamicol. The K_d values were 3.5 and 178.7 nM for the high- and low-affinity binding sites, respectively. The corresponding B_{max} values were 36.6 and 156.0 pmol/g, respectively. The mean affinity and density values for 5 experiments are reported in the text.

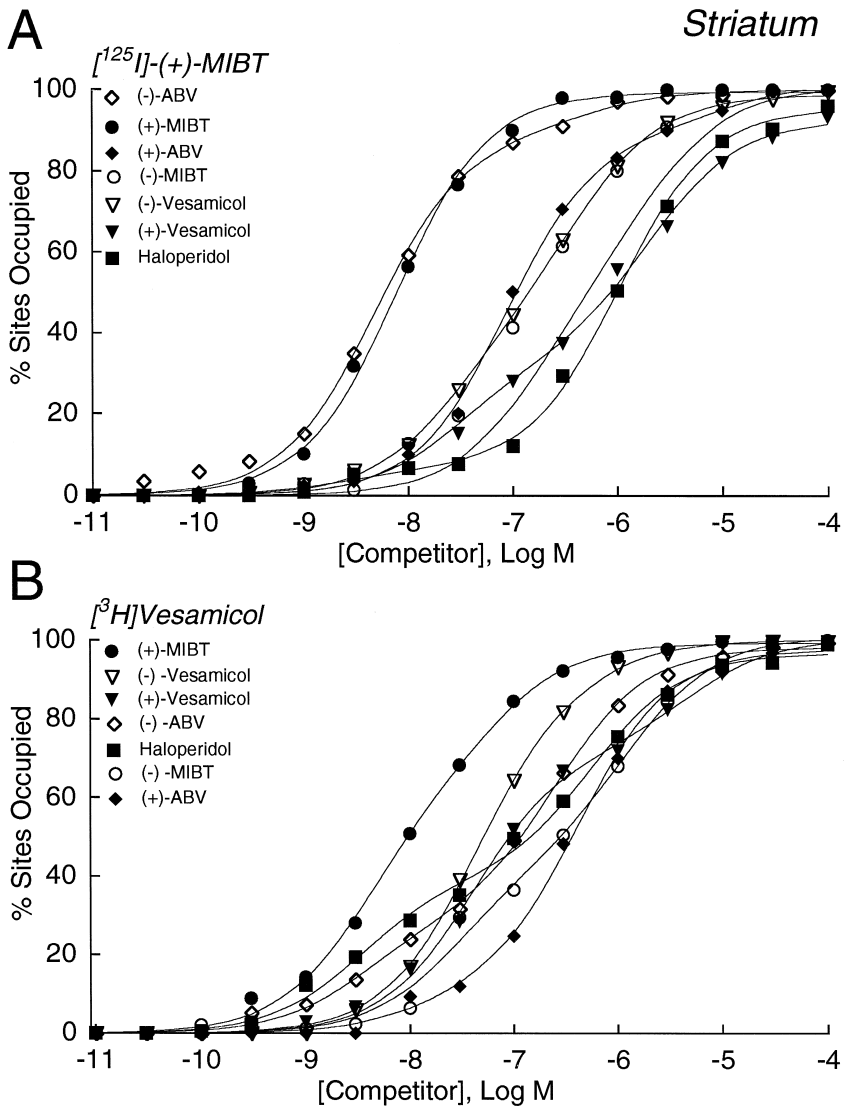

Fig. 4. Pharmacological characterization of (A) (+)-[^{125}I]MIBT and (B) [^{3}H]vesamicol binding to striatum. Drugs known to label the vesicular acetylcholine transporter or σ receptor ligands were used to compete for (+)-[^{125}I]MIBT (0.07 nM) or [^{3}H]vesamicol (4 nM) binding sites in membrane homogenates from the striatum. Nonspecific binding was defined with 1 μM (+)-*meta*-iodobenzyltrozamicol. Each datum in the figure represents the average of 2–4 individual experiments each performed in triplicate. The stereoselectivity and the rank order of potency illustrated is indicative of labeling to the vesicular acetylcholine transporter.

of (+)-[^{125}I]MIBT binding. In contrast, the σ receptor ligands haloperidol and (+)- and (−)-pentazocine displayed significantly lower potency at this site. Among the vesamicol analogues, interaction with this site was characterized by a high degree of stereoselectivity similar to that observed with (−)-[^{3}H]vesamicol in *Torpedo* synaptic vesicles (Rogers et al., 1993). Specifically, (−)-vesamicol was five times more potent than (+)-vesamicol while (−)-5-aminobenzovesamicol, (+)-*meta*-iodobenzyltrozamicol and (+)-*para*-fluorobenzyltrozamicol were 8- to 16-fold more potent than their corresponding antipodes. (The apparent reversal of stereoselectivity associated with MIBT and *para*-fluorobenzyltrozamicol has been reported in previous studies (Efange et al., 1993b, 1994a) and is associated with the introduction of a nitrogen atom into the cyclohexyl moiety of vesamicol. Presumably, the absolute configurations of the carbons bearing the critical amino and hydroxyl groups of (−)-vesamicol and *meta*-iodobenzyltrozamicol are the same.) Consistent with previous studies of (−)-[^{3}H]vesamicol binding to *Torpedo* synaptic vesicles, (−)-5-aminobenzovesamicol ($K_i = 6.1 \pm 1.1$ nM) and (+)-*meta*-iodobenzyltrozamicol ($K_i = 8.9 \pm 3.2$ nM) emerged as the most potent inhibitors of (+)-[^{125}I]MIBT binding while (−)-vesamicol ($K_i = 160 \pm 36$ nM) displayed moderate potency. At concentrations as high as 200 mM, acetylcholine did not inhibit the binding of (+)-[^{125}I]MIBT. The resulting rank order of potency ((+)-*meta*-iodobenzyltrozamicol = (−)-5-aminobenzovesamicol > (+)-*para*-fluorobenzyltrozamicol > (+)-5-aminobenzovesamicol > (−)-*meta*-iodobenzyltrozamicol = (−)-

Table 1
Pharmacology of vesamicol analogues and σ receptor ligands in monkey striatum

Competitor	[^{125}I]MIBT		[^{3}H]Vesamicol	
	K_i (nM)	n_H	K_i (nM)	n_H
Vesamicol analogues				
(−)-ABV	6.1 ± 1.1	0.69	176.6 ± 0.2	0.71
(+)-ABV	82.7 ± 3.0	0.86	539.5 ± 61.9	0.78
(−)-FBT	335.2 ± 146.4	0.80	223.7 ± 22.1	0.77
(+)-FBT	42.0 ± 5.7	0.77	9.0 ± 1.2	0.82
(−)-MIBT	146.9 ± 15.0	0.79	474.7 ± 30.0	0.73
(+)-MIBT	8.9 ± 3.2	1.10	17.5 ± 4.3	0.71
(−)-Vesamicol	154.6 ± 35.8	0.72	53.1 ± 16.3	0.92
(+)-Vesamicol	689.5 ± 357.3	0.58	115.4 ± 35.8	0.64
σ ligands				
Haloperidol	1022.0 ± 295.6	0.74	207.7 ± 6.7	0.53
(−)-Pentazocine	6562.6 ± 1864.6	0.64	1471.4 ± 489.4	0.86
(+)-Pentazocine	7026.6 ± 3541.0	0.65	1824.3 ± 492.9	0.84

The data shown are the mean ± S.E. of 2–4 independent determinations each performed in triplicate. Nonspecific binding was determined using 1 μM (+)-MIBT. The K_i values and Hill coefficients were determined using EBDA (DRUG)/LIGAND.

vesamicol ≥ (−)-*para*-fluorobenzyltrozamicol ≥ (+)-vesamicol ≥ haloperidol > (−)-pentazocine = (+)-pentazocine) bears striking similarity to that obtained from the inhibition of [^{3}H](−)-vesamicol binding to purified *Torpedo* synaptic vesicles.

A qualitatively similar pharmacological profile was demonstrated for the inhibition of [^{3}H]vesamicol binding to primate striatal membranes (Fig. 4B and Table 1). Competition binding for [^{3}H](−)-vesamicol was conducted at a concentration of 5 nM. Using the K_d and B_{max} values reported for [^{3}H](−)-vesamicol binding to rat brain membrane homogenates (Meyer et al., 1993), we have calculated that at this concentration the high- and low-affinity sites accounted for 58% and 42% of the bound [^{3}H](−)-vesamicol, respectively. Due to the low specific activity of [^{3}H](−)-vesamicol, we were unable to use a lower concentration of radioligand to selectively label the high-affinity site. Nevertheless, we find that vesamicol analogues emerged as the most potent inhibitors of [^{3}H](−)-vesamicol binding to striatal membranes. Moreover, the inhibition was characterized by a significant degree of stereoselectivity: (−)-vesamicol was twice as potent as (+)-vesamicol while (−)-5-aminobenzovesamicol, (+)-*meta*-iodobenzyltrozamicol and (+)-*para*-fluorobenzyltrozamicol were 3–27 times more potent than the corresponding antipodes. However, qualitative differences were also evident. For example, (−)-5-aminobenzovesamicol, the most potent vesicular acetylcholine transporter ligand reported in *Torpedo* (Rogers et al., 1993), was found to be a weak inhibitor of [^{3}H]vesamicol binding in monkey striatal membranes, while haloperidol, a nonselective σ ligand, displayed moderate potency against this radioligand. Lastly, Hill coefficients for all compounds used in the competition studies were significantly less than unity.

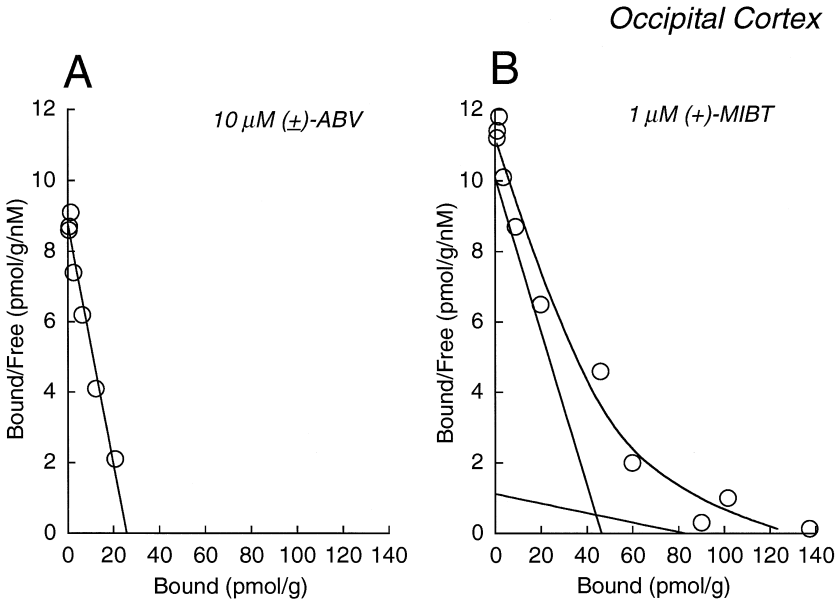

Fig. 5. Cold saturation analysis of (+)-[^{125}I]MIBT binding to occipital cortex. Membrane homogenates from the occipital cortex were incubated with (+)-[^{125}I]MIBT (0.07 nM) in the presence of increasing concentrations of unlabeled (+)-*meta*-iodobenzyltrozamicol for 1 h at 25°C. Shown here is a representative experiment assayed in triplicate. The data were analyzed with the EBDA/LIGAND program for binding analysis. (A) Rosenthal plot with the nonspecific binding defined using 10 μM (±) ABV demonstrates a single site with a K_d value of 2.9 nM and a B_{max} value of 25.4 pmol/g. (B) Rosenthal plot obtained when nonspecific binding was defined using 1 μM (+)-*meta*-iodobenzyltrozamicol. The K_d values were 4.6 and 74.9 nM for the high- and low-affinity binding sites, respectively. The corresponding B_{max} values were 46.4 and 82.8 pmol/g tissue, respectively. The mean affinity and density values for 6 individual experiments are reported in the text.

3.2. Characterization of (+)-[^{125}I]MIBT binding in primate occipital cortex: comparison with [^{3}H]vesamicol binding

Saturation plots of (+)-[^{125}I]MIBT binding to primate occipital cortex are shown in Fig. 5. As observed with striatal membranes, the shape of the Rosenthal plot was dependent on the vesamicol analogue that was used to define the nonspecific binding. When the latter was defined with 10 μM (±)-5-aminobenzovesamicol, a linear Rosenthal plot was obtained, suggesting a single high-affinity binding site (Fig. 5A). The associated mean K_d and B_{max} values obtained from six independent determinations were 4.6 ± 1.1 nM and 32 ± 7.0 pmol/g tissue, respectively. However, when the nonspecific binding component was determined with 1 μM *meta*-iodobenzyltrozamicol, the Rosenthal plot was curvilinear (Fig. 5B), thereby revealing a high- (K_d = 3.3 ± 1.0 nM) and low-affinity (K_d = 114 ± 59 nM) site. The densities associated with these two sites were 30 ± 12 and 97 ± 12 pmol/g, respectively (n = 6; $p < 0.01$).

Pharmacological characterization of the binding of (+)-[^{125}I]MIBT to occipital cortex membranes is illustrated in Fig. 6A and summarized in Table 2. Over 90% of the bound (+)-[^{125}I]MIBT occupied the high-affinity site, while less than 10% occupied the low-affinity site in the primate occipital cortex. The most potent inhibitors of (+)-[^{125}I]MIBT binding were vesamicol analogues. For (+)-*meta*-iodobenzyltrozamicol and (+)-*para*-fluorobenzyltrozamicol, the K_i values for inhibition of (+)-

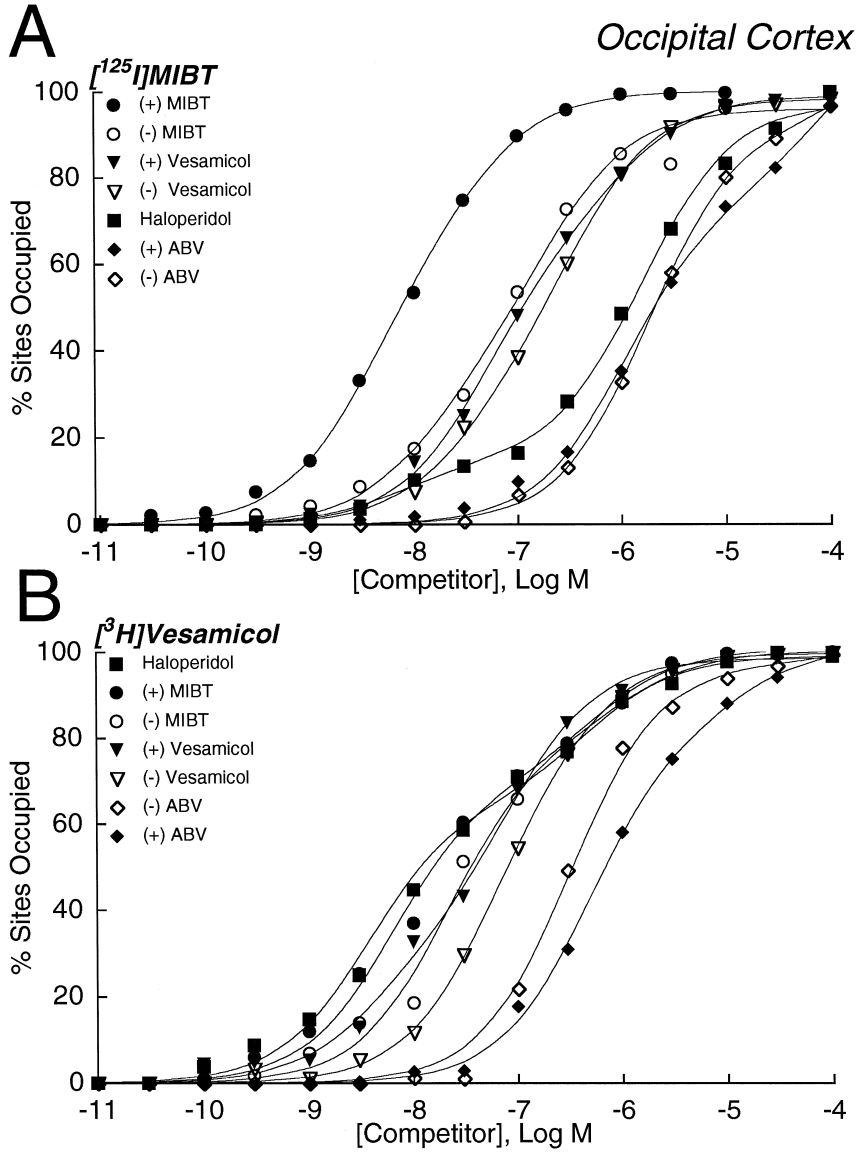

Fig. 6. Pharmacological characterization of (A) (+)-[^{125}I]MIBT and (B) [^{3}H]vesamicol binding to occipital cortex. Drugs known to label the vesicular acetylcholine transporter or σ receptor ligands were used to compete for (+)-[^{125}I]MIBT (0.07 nM) or [^{3}H]vesamicol (4 nM) binding sites in membrane homogenates from the occipital cortex. Nonspecific binding was defined using 1 μM (+)-*meta*-iodobenzyltrozamicol. Each curve shown is the average of 2–4 independent experiments each performed in triplicate. Note the significant decrease in the inhibitory potency of (−)-ABV.

Table 2
Pharmacology of vesamicol analogues and σ receptor ligands in monkey occipital cortex

Competitor	[^{125}I]MIBT		[^{3}H]Vesamicol	
	K_i (nM)	nH	K_i (nM)	n_H
Vesamicol analogues				
(−)-ABV	806.3 ± 290.6	0.80	286.4 ± 55.0	0.80
(+)-ABV	1607.1 ± 735.1	0.85	964.8 ± 304.3	0.84
(−)-FBT	262.4 ± 116.7	0.69	30.3 ± 1.3	0.73
(+)-FBT	30.8 ± 9.5	0.87	12.3 ± 2.1	0.81
(−)-MIBT	87.0 ± 24.7	0.77	58.0 ± 27.7	0.67
(+)-MIBT	9.4 ± 3.5	0.87	41.4 ± 11.9	0.61
(−)-Vesamicol	202.6 ± 52.1	0.82	91.3 ± 28.4	0.90
(+)-Vesamicol	135.4 ± 26.5	0.68	58.6 ± 14.8	0.74
σ ligands				
Haloperidol	948.6 ± 355.9	0.83	9.6 ± 5.7	0.50
(−)-pentazocine	1676.0 ± 540.6	0.70	588.9 ± 388.9	0.80
(+)-pentazocine	3396.8 ± 492.0	0.52	835.6 ± 158.3	0.71

The data shown are the mean ± S.E. of 2–4 independent determinations each performed in triplicate. Nonspecific binding was determined using 1 μM (+)-MIBT. The K_i values and Hill coefficients were determined using EBDA (DRUG)/LIGAND.

[^{125}I]MIBT binding were 9.4 ± 3.5 and 31 ± 10 nM, respectively (Table 2). In contrast, the corresponding antipodes displayed 9-fold lower potency at this site. However, the rank order of potencies observed in the occipital cortex differed in many respects from that derived from the striatum, particularly with respect to stereoselectivity and the potency of (−)-5-aminobenzovesamicol. The latter compound, surprisingly, was among the weakest inhibitors of (+)-[^{125}I]MIBT binding, along with the σ receptor ligands haloperidol, (+)- and (−)-pentazocine. In addition, there was little evidence of stereoselectivity in the interaction of 5-aminobenzovesamicol and vesamicol with the high-affinity site in the occipital cortex.

The pharmacology of [^{3}H]vesamicol binding was assessed in a similar manner in the occipital cortex (Fig. 6B). In contrast to the striatum, the rank orders of potencies obtained for these two radiotracers in the occipital cortex were completely discordant. For the inhibition of [^{3}H](−)-vesamicol, (+)-*para*-fluorobenzyltrozamicol and haloperidol emerged as the most potent compounds, while (+)-5-aminobenzovesamicol and (+) and (−)-pentazocine displayed the lowest potency. Furthermore, the interaction of test compounds with [^{3}H](−)-vesamicol was not characterized by stereoselectivity. Finally, all Hill coefficients were less than unity as observed in the striatum.

4. Discussion

(+)-*meta*-Iodobenzyltrozamicol is a potent vesicular acetylcholine transporter ligand (Efange et al., 1993a,b). In *Torpedo* synaptic vesicles, the binding of this ligand exhibits a high degree of stereoselectivity (K_i: (+)-*meta*-iodobenzyltrozamicol, 0.06 ± 0.01 nM; (−)-*meta*-iodobenzyltrozamicol, 8.0 ± 3.2 nM; Efange et al., 1994b). In contrast to its subnanomolar affinity for the vesicular acetylcholine transporter in *Torpedo*, *meta*-iodobenzyltrozamicol exhibits relatively low affinity at σ sites in the rat brain (Efange et al., 1995). Moreover, the distribution of this ligand in vivo corresponds to known patterns of central cholinergic innervation (Efange et al., 1993b), suggesting that radiolabeled *meta*-iodobenzyltrozamicol is potentially useful for mapping cholinergic innervation in vitro or in vivo. On the basis of these encouraging preliminary studies, further characterization of this ligand was undertaken in the primate brain in vitro. To fully assess the potential utility of (+)-[^{125}I]MIBT, the pharmacological profile of this radioligand was compared to that of (−)-[^{3}H]vesamicol, the prototypical ligand for the vesicular acetylcholine transporter.

In the present study, we find that the binding of (+)-[^{125}I]MIBT to primate striatum and occipital cortex is saturable and reversible. Association and dissociation of this ligand are both rapid and biphasic. In saturation binding studies, (+)-[^{125}I]MIBT labels a single high-affinity site in the striatum ($K_d = 4.4 \pm 0.7$ nM, $B_{max} = 41 \pm 7$ pmol/g) when (±)-5-aminobenzovesamicol (10 μM) is used to define the background. In contrast, two classes of binding sites, one high- ($K_d = 3.9 \pm 0.5$ nM, $B_{max} = 38 \pm 11$ pmol/g) and one low-affinity ($K_d = 160 \pm 70$ nM, $B_{max} = 160 \pm 20$ pmol/g), are revealed when the nonspecific binding is defined with 1 μM (*meta*-iodobenzyl)trozamicol. This difference suggests that 10 μM (±)-5-aminobenzovesamicol blocks only one of two *meta*-iodobenzyltrozamicol binding sites. Saturation of membranes from the occipital cortex by (+)-[^{125}I]MIBT exhibits a similar dependence on the compound used to determine nonspecific binding.

Competition studies with (+)-[^{125}I]MIBT in striatum primarily monitored the high-affinity binding site. A distinctive feature of the rank order of potencies obtained from these studies is that vesamicol and its analogues are more effective in competing for this high-affinity site than are the σ ligands haloperidol and pentazocine. Furthermore, the vesamicol analogues exhibit a high degree of stereoselectivity similar to that observed for the inhibition of (−)-[^{3}H]vesamicol binding to the vesicular acetylcholine transporter in *Torpedo* synaptic vesicles. Taken together, the foregoing suggest that the high-affinity (+)-[^{125}I]MIBT binding site is localized on the vesicular acetylcholine transporter.

Although low concentrations of (+)-*meta*-iodobenzyltrozamicol appear to bind primarily to the vesicular acetylcholine transporter in striatal membranes, we note that the dissociation constant obtained from the present study is approximately 70-fold higher than that obtained from competition assays with (−)-[^{3}H]vesamicol in *Torpedo* synaptic vesicles. Since comparable K_d values for (−)-[^{3}H]vesamicol have been obtained from the cloned

human (Varoqui and Erickson, 1996) and *Torpedo* (Rogers et al., 1993) vesicular acetylcholine transporter, we suggest that the higher K_d obtained for (+)-[^{125}I]MIBT in the present study probably reflects differences in tissue preparation. While highly purified synaptic vesicles have been used to obtain dissociation constants for (+)-*meta*-iodobenzyltrozamicol and (−)-vesamicol in *Torpedo*, the present study utilized a membrane homogenate.

Competition studies with (+)-[^{125}I]MIBT in the occipital cortex revealed some parallels with the striatum. Specifically, vesamicol analogues were found to be the most potent inhibitors of (+)-[^{125}I]MIBT binding while the σ ligands were the least potent. In addition, the binding of *meta*-iodobenzyltrozamicol and *para*-fluorobenzyltrozamicol was characterized by a high degree of stereoselectivity similar to that observed in the monkey striatum and *Torpedo* synaptic vesicles. However, the rank order of potencies obtained in the occipital cortex was significantly different from that observed in the striatum. Notable among these differences was the 100-fold drop in the potency of (−)-5-aminobenzovesamicol, one of the most potent vesicular acetylcholine transporter ligands ever reported. Another important difference was the loss of stereoselectivity in the interaction of this site with 5-aminobenzovesamicol and vesamicol.

The relative amounts of vesicular acetylcholine transporter in rat striatum and cortex have been estimated immunochemically by Western blot. Although the ratio was not quantitated, as estimated visually the amount of vesicular acetylcholine transporter in striatal membranes is about 10-fold greater than the amount in cortical membranes (Gilmor et al., 1996). Staining for vesicular acetylcholine transporter protein and mRNA in cell bodies, puncta and fibers of rat brain sections supports this estimate (Schafer et al., 1994; Erickson et al., 1994; Roghani et al., 1994; Gilmor et al., 1996; Weihe et al., 1996). Rat and monkey cortex contain similar amounts of vesicular acetylcholine transporter immunoreactivity (Schafer et al., 1995). In addition, comparable estimates have been obtained for choline acetyltransferase activity in human (Araujo et al., 1988) and rat (Stavinoha et al., 1974; Kuczenski et al., 1975) brain. Using the 10:1 ratio and assuming that all of the high-affinity binding of (+)-[^{125}I]MIBT in monkey striatum is to the vesicular acetylcholine transporter, we can estimate that the stained vesicular acetylcholine transporter accounts for no more than 5 pmol/g of monkey cortex of the estimated 25–46 pmol/g tissue associated with high-affinity binding in cortex. Thus, there must be two high-affinity binding sites for (+)-[^{125}I]MIBT in the occipital cortex.

While this analysis suggests that only 10–20% of the high-affinity binding of (+)-[^{125}I]MIBT in cortical membranes could be due to immunostained vesicular acetylcholine transporter, Efange et al. (1997) have recently demonstrated that Alzheimer's patients suffer about a 50% loss of (+)-[^{125}I]MIBT binding to cortical membranes relative to age-matched controls. The large discrepancy between the latter number and the 5–10% loss of cortical binding of (+)-[^{125}I]MIBT predicted for a 50% loss of cholinergic terminals (assuming that the major (+)-binding site is noncholinergic) could be due the existence of vesicular acetylcholine transporter isoforms. Recent cloning of mammalian vesicular acetylcholine transporter cDNAs has revealed a single gene encoding the vesicular acetylcholine transporter (Erickson et al., 1994; Bejanin et al., 1994; Roghani et al., 1994). However, while the coding sequence for the gene is continuous, at least 4 types of vesicular acetylcholine transporter mRNAs (V1a, V1b, V2, V3), which are presumed to result from differential promoter regulation of transcription of the vesicular acetylcholine transporter gene have been reported (Bejanin et al., 1994; Cervini et al., 1995). Moreover, there is little information available about the structure of the protein itself and its immunogenic homogeneity. This leaves open the possibility that multiple forms of the vesicular acetylcholine transporter exist that display different drug binding characteristics, and that the atypical pharmacological profile associated with the high-affinity binding of (+)-[^{125}I]MIBT in the occipital cortex may represent a variant of the vesicular acetylcholine transporter distinct from that associated with cholinergic interneurons of the striatum. Such differences may not be altogether surprising since the cholinergic neurons in the striatum are intrinsic to this structure, while the majority of cholinergic innervation to the cortex originates from the basal forebrain nucleus (Mesulam et al., 1983) and is therefore extrinsic.

(−)-[^{3}H]Vesamicol was studied in parallel competition experiments using membranes from striatum and occipital cortex. Significant binding to low-affinity sites probably occurred in both cases because a relatively high reduced concentration (concentration divided by the dissociation constant) of (−)-[^{3}H]vesamicol was used. This was required because of the lower specific radioactivity of ^{3}H compared to that of ^{125}I. The labelling of both high and low-affinity sites by (−)-[^{3}H]vesamicol may be sufficient to alter the pharmacological profile. The apparent K_i values obtained for (−)-vesamicol in monkey striatum and occipital cortex were 53 nM and 91 nM, respectively. These values are threefold lower than those obtained by Meyer et al. (1993) in rat brain. In the monkey striatum, the pharmacological profile of the high-affinity binding site for (−)-[^{3}H]vesamicol bears a strong resemblance to that of the vesicular acetylcholine transporter in *Torpedo* synaptic vesicles. However, there are some notable differences. While (−)-5-aminobenzovesamicol is 150 times more potent than (−)-vesamicol in *Torpedo* synaptic vesicles (Rogers et al., 1993), in the current study (−)-vesamicol appears to be threefold more potent than (−)-5-aminobenzovesamicol. Moreover, haloperidol, a potent σ receptor ligand, appears to be equipotent with (−)-5-aminobenzovesamicol. In contrast to the striatum, competition studies with [^{3}H]vesamicol in occipital cortex yielded

little evidence of stereoselectivity with vesamicol analogues and an inappropriate rank order of potencies. Moreover, haloperidol, a potent σ receptor ligand, was found to be the most potent inhibitor of [^{3}H]vesamicol binding in the cortex. Consequently, we conclude that the binding of [^{3}H]vesamicol in the monkey striatum reflects both the vesicular acetylcholine transporter and σ receptors; however, in the cortex, this radioligand binds primarily to σ receptors. This conclusion is consistent with previous reports showing that haloperidol can displace (−)-[^{3}H]vesamicol from *Torpedo* synaptic vesicles (Kaufman et al., 1989), rat brain slices (Altar and Marien, 1988) and human cerebral cortex (Efange et al., 1992). Moreover, these results are consistent with the marginal selectivity of (−)-vesamicol for the vesicular acetylcholine transporter relative to the σ receptor (Efange et al., 1994b). Taken together, the foregoing strongly suggests that (+)-[^{125}I]MIBT is superior to (−)-[^{3}H]vesamicol.

In summary, *meta*-iodobenzyltrozamicol is a reliable probe for the vesicular acetylcholine transporter in monkey striatum, but its binding behavior in monkey cortex cannot be fully explained by a single vesicular acetylcholine transporter isoform. In view of our limited knowledge of this transporter, a more complete characterization of possible regional differences in vesicular acetylcholine transporter structure is clearly desirable. Since the existence of multiple forms of vesicular acetylcholine transporter in the mammalian cortex would complicate the interpretation of radioligand binding studies of vesicular acetylcholine transporter ligands, thorough in vitro characterization of new vesicular acetylcholine transporter ligands prior to their use as imaging agents in the study of central cholinergic function is strongly indicated.

Acknowledgements

This work was supported by the NIH under grant number NS28711 (SMNE), AG13621 (SMNE) and NS15047 (SMP).

References

Altar, C.A., Marien, M.R., 1988. [^{3}H]Vesamicol binding in brain: Autoradiographic distribution, pharmacology, and effects of cholinergic lesions. Synapse 2, 486–493.

Anderson, D.C., King, S.C., Parsons, S.M., 1983. Pharmacological characterization of the acetylcholine transport system in purified *Torpedo* electric organ synaptic vesicles. Mol. Pharmacol. 24, 48–54.

Araujo, D.M., Lapchak, P.A., Robitaille, Y., Gauthier, S., Quirion, R., 1988. Differential alteration of various cholinergic markers in cortical and subcortical regions of human brain in Alzheimer's disease. J. Neurochem. 50, 1914–1923.

Bahr, B.A., Parsons, S.M., 1986a. Acetylcholine transport and drug inhibition kinetics in *Torpedo* synaptic vesicles. J. Neurochem. 46, 1214–1218.

Bahr, B.A., Parsons, S.M., 1986b. Demonstration of a receptor in *Torpedo* synaptic vesicles for the acetylcholine storage blocker L-*trans*-2-(4-phenyl[3,4-^{3}H]-piperidino)cyclohexanol. Proc. Natl. Acad. Sci. USA 83, 2267–2270.

Bejanin, S., Cervini, R., Mallet, J., Berrard, S., 1994. A unique gene organization for two cholinergic markers, choline acetyltransferase and a putative vesicular transporter of acetylcholine. J. Biol. Chem. 269, 21944–21947.

Cervini, T., Houhou, L., Pradat, P.F., Bejanin, S., Mallet, J., Berrard, S., 1995. Specific vesicular acetylcholine transporter promoters lie within the first intron of the rat choline acetyltransferase gene. J. Biol. Chem. 270, 24654–24657.

Efange, S.M.N., Mash, D.C., Basile, M., Pablo, J., Kung, H.F., Michelson, R.H., Thomas, J.R., 1992. The vesamicol receptor (VR) radioligand selectivity and the detection of central cholinergic hypofunction. J. Label. Compd. Radiopharm. (Spec. Symp. Issue) 32, 311–312.

Efange, S.M.N., Khare, A., Parsons, S.M., Bau, R., Metzenthin, T., 1993a. Non-symmetrical bipiperidyls as inhibitors of vesicular acetylcholine storage. J. Med. Chem. 36, 985–989.

Efange, S.M.N., Michelson, R.H., Khare, A.B., Thomas, J.R., 1993b. Synthesis and tissue distribution of (*m*-[^{125}I]iodobenzyl)trozamicol ([^{125}I]MIBT): Potential radioligand for mapping central cholinergic innervation. J. Med. Chem. 36, 1754–1760.

Efange, S.M.N., Mach, R.H., Khare, A.B., Michelson, R.H., Nowak, P.A., Evora, P.H., 1994a. *p*-[^{18}F]Fluorobenzyltrozamicol ([^{18}F]FBT): Molecular decomposition-reconstitution approach to vesamicol receptor radioligands for positron emission tomography. Appl. Radiat. Isot. 45, 465–472.

Efange, S.M.N., Khare, A.B., Foulon, C., Akella, S.K., Parsons, S.M., 1994b. Spirovesamicols: Conformationally restricted analogs of 2-(4-phenylpiperidino)-cyclohexanol (vesamicol, AH5183) as potential modulators of presynaptic cholinergic function. J. Med. Chem. 37, 2574–2582.

Efange, S.M.N., Mach, R.H., Smith, C.R., Khare, A.B., Foulon, C., Akella, S.K., Childers, S.R., Parsons, S.M., 1995. Vesamicol analogues as σ ligands: Molecular determinants of selectivity at the vesamicol receptor. Biochem. Pharmacol. 49, 791–797.

Efange, S.M.N., Garland, E., Staley, J.K., Khare, A.B., Mash, D.C., 1997. Vesicular acetylcholine transporter (VAChT) density and Alzheimer's disease. Neurobiol. Aging, in press.

Erickson, J.D., Varoqui, H., Schafer, M.K.H., Modi, W., Diebler, M.F., Weihe, E., Rand, J., Eiden, L.E., Bonner, T.I., Usdin, T.B., 1994. Functional identification of a vesicular acetylcholine transporter and its expression from a 'cholinergic' gene locus. J. Biol. Chem. 269, 21929–21932.

Gilmor, M.L., Nash, N.R., Roghani, A., Edwards, R.H., Yi, H., Hersch, S.M., Levey, A.I., 1996. Expression of the putative vesicular acetylcholine transporter in rat brain and localization in cholinergic synaptic vesicles. J. Neurosci. 16, 2179–2190.

Haigh, J.R., Noremberg, K., Parsons, S.M., 1994. Acetylcholine active transport by rat brain synaptic vesicles. Neuroreport 5, 773–776.

Holley, L.A., Miller, J.A., Chmielewski, P.A., Dudchenko, P., Sarter, M., 1993. Interactions between the effects of basal forebrain lesions and chronic treatment with MDL 26,479 on learning and markers of cholinergic transmission. Brain Res. 610, 181–193.

Kaufman, R., Rogers, G.A., Fehlmann, C., Parsons, S.M., 1989. Fractional vesamicol receptor occupancy and acetylcholine active transport inhibition in synaptic vesicles. Mol. Pharmacol. 36, 452–458.

Kilbourn, M.R., Jung, Y.-W., Haka, M.S., Gildersleeve, D.L., Kuhl, D.E., Wieland, D.M., 1990. Mouse brain distribution of a carbon-11 labeled vesamicol derivative: Presynaptic marker of cholinergic neurons. Life Sci. 47, 1955–1963.

Kish, S.J., Distefano, L.M., Dozic, S., Robitaille, Y., Rajput, A., Deck, J.H.N., Hornykiewicz, O., 1990. [^{3}H]Vesamicol binding in human brain cholinergic deficiency disorders. Neurosci. Lett. 117, 347–352.

Kuczenski, R., Segal, D.S., Marshall, A.J., 1975. Regional and subcellu-

lar distribution and kinetic properties of rat brain choline acetyltransferase – Some functional considerations. J. Neurochem. 24, 39–45.

Kuhl, D.E., Koeppe, R.A., Fessler, J.A., Minoshima, S., Ackermann, R.J., Carey, J.E., Gildersleeve, D.L., Frey, K.A., Wieland, D.M., 1994. In vivo mapping of cholinergic neurons in the human brain using SPECT and IBVM. J. Nucl. Med. 35, 405–410.

Marien, M.R., Parsons, S.M., Altar, C.A., 1987. Quantitative autoradiography of brain binding sites for the vesicular acetylcholine transport blocker 2-(4-phenylpiperidino) cyclohexanol (AH5183). Proc. Natl. Acad. Sci. USA 84, 876–880.

Mesulam, M.M., Mufson, E.J., Levey, A.I., Wainer, B.H., 1983. Cholinergic innervation of cortex by the basal forebrain: Cytochemistry and cortical connections of the septal area, diagonal band nucleus, nucleus basalis (substantia inominata) and hypothalamus in the rhesus monkey. J. Comp. Neurol. 214, 170–197.

Meyer, E.M., Bryant, S.O., Wang, R.H., Watson, R.J., 1993. Characterization of [^{3}H]vesamicol binding in rat brain preparations. Neurochem. Res. 18, 1067–1073.

Mulholland, G.K., Jung, Y.-W., Sherman, P.S., Pisani, T.L., Kuhl, D.E., Wieland, D.M., Kilbourn, M.R., 1992. Efficient one-step synthesis of (−)-[^{18}F]fluoroethoxybenzovesamicol (FEOBV): A new tracer for mapping cholinergic neurons in vivo. J. Label. Compd. Radiopharm. (Spec. Symp. Issue) 32, 487.

Quirion, R., 1987. Characterization and autoradiographic distribution of hemicholinium-3 high-affinity uptake sites in mammalian brain. Synapse 1, 293–303.

Ricny, J., Whittaker, V.P., 1993. Vesamicol blocks the recovery, by recycling cholinergic electromotor synaptic vesicles of the biophysical characteristics of the reserve population. Biochim. Biophys. Acta 1148, 234–238.

Rogers, G.A., Parsons, S.M., 1990. Persistent occupation of the vesamicol receptor. NeuroReport 1, 22–25.

Rogers, G.A., Parsons, S.M., 1993. Photoaffinity labeling of the vesamicol receptor of cholinergic synaptic vesicles. Biochemistry 32, 8596–8601.

Rogers, G.A., Parsons, S.M., Anderson, D.C., Nilsson, L.M., Bahr, B.A., Kornreich, W.D., Kaufman, R., Jacobs, R.S., Kirtman, B., 1989. Synthesis, in vitro acetylcholine-storage-blocking activities, and biological properties of derivatives and analogues of trans-2-(4-phenylpiperidino)cyclohexanol (vesamicol). J. Med. Chem. 32, 1217–1230.

Rogers, G.A., Stone-Elander, S., Eriksson, L., Ingvar, M., Parsons, S.M., Widen, L., 1992. [^{18}F]Vesamicol derivatives for in vivo evaluation as tracers for cholinergic synaptic vesicles. J. Label. Compd. Radiopharm. (Spec. Symp. Issue) 32, 486.

Rogers, G.A., Kornreich, W.D., Hand, K., Parsons, S.M., 1993. Kinetic and equilibrium characterization of vesamicol receptor–ligand complexes with picomolar dissociation constants. Mol. Pharmacol. 44, 633–641.

Roghani, A., Feldman, J., Kohan, S.A., Shirzadi, A., Gundersen, C.B., Brecha, N., Edwards, R.H., 1994. Molecular cloning of a putative vesicular transporter for acetylcholine. Proc. Natl. Acad. Sci. USA 91, 10620–10624.

Ruberg, M., Mayo, W., Brice, A., Duyckaerts, C., Hauw, J.J., Simon, H., LeMoal, M., Agid, Y., 1990. Choline acetyltransferase activity and [^{3}H]vesamicol binding in the temporal cortex of patients with Alzheimer's disease, Parkinson's disease, and rats with basal forebrain lesions. Neuroscience 35, 327–333.

Schafer, M.K.-H., Weihe, E., Varoqui, H., Eiden, L.E., Erickson, J.D., 1994. Distribution of the vesicular acetylcholine transporter (VAChT) in the central and peripheral nervous systems of the rat. J. Mol. Neurosci. 5, 1–26.

Schafer, M.K.-H., Weihe, E., Erickson, J.D., Eiden, L.E., 1995. Human and monkey cholinergic neurons visualized in paraffin-embedded tissues by immunoreactivity for VAChT, the vesicular acetylcholine transporter. J. Mol. Neurosci. 6, 225–235.

Shiba, K., Mori, H., Matsuda, H., Ichikawa, A., Tonami, N., 1996. Radioiodinated (−)-2-[4-(3-iodophenyl) piperidino]cyclohexanol: A potential radioligand for mapping presynaptic cholinergic neurons. Nucl. Med. Commun. 17, 485–492.

Stavinoha, W.B., Weintraub, S.T., Modak, A.T., 1974. Regional concentrations of choline and acetylcholine in the rat brain. J. Neurochem. 23, 885–886.

Van Dort, M.E., Jung, Y.-W., Gildersleeve, D.L., Hagen, C.A., Kuhl, D.E., Wieland, D.M., 1993. Synthesis of the ^{123}I- and ^{125}I-labeled cholinergic nerve marker (−)-5-iodobenzovesamicol. Nucl. Med. Biol. 20, 929–937.

Varoqui, H., Erickson, J.D., 1996. Active transport of acetylcholine by the human vesicular acetylcholine transporter. J. Biol. Chem. 271, 27229–27232.

Weihe, E., Tao-Cheng, J.H., Schafer, M.K.H., Erickson, J.D., Eiden, L.E., 1996. Visualization of the vesicular acetylcholine transporter in cholinergic nerve terminals and its targeting to a specific population of small synaptic vesicles. Proc. Natl. Acad. Sci. USA 93, 3547–3552.